Appl. Sci. **2015**, *5*, 566-574; doi:10.3390/app5030566

OPEN ACCESS

applied sciences

ISSN 2076-3417

www.mdpi.com/journal/applsci

Article

Q-Switched Operation with Carbon-Based Saturable Absorbers in a Nd:YLF Laser

Rosa Weigand [1,*], Margarita Sánchez Balmaseda [2] and José Manuel Guerra Pérez [1]

[1] Departamento de Óptica, Facultad de Ciencias Físicas, Universidad Complutense de Madrid, Avda. Complutense s/n, 28040 Madrid, Spain; E-Mail: jmguerra@fis.ucm.es

[2] Departamento de Física Aplicada III, Facultad de Informática, Universidad Complutense de Madrid, Avda. Prof. Santesmases s/n, 28040 Madrid, Spain; E-Mail: msanchez@fis.ucm.es

* Author to whom correspondence should be addressed; E-Mail: weigand@fis.ucm.es; Tel.: +34-91-394-4508; Fax: +34-91-394-4683.

Academic Editor: Malte C. Kaluza

Received: 17 August 2015 / Accepted: 1 September 2015 / Published: 11 September 2015

Abstract: We have numerically studied the influence of the absorption modulation depth of carbon-based saturable absorbers (graphene and carbon nanotubes (CNTs)) on the Q-switched regime of a diode-pumped Nd:YLF laser. A short-length cavity was used with an end mirror on which CNTs or mono- or bi-layer graphene were deposited, forming a saturable absorber mirror (SAM). Using a standard model, the generated energy per pulse was calculated, as well as the pulse duration and repetition rate. The results show that absorbers with higher modulation depths, *i.e.*, graphene, deliver higher energy pulses at lower repetition rates. However, the pulse duration did not have a monotonic behavior and reaches a minimum for a given low value of the modulation depth typical of CNTs.

Keywords: diode-pumped lasers; Q-switched Nd:YLF laser; mode-locked Nd:YLF; graphene saturable absorber; carbon nanotube saturable absorber

1. Introduction

The passive Q-switched and mode locking operation of lasers using saturable absorbers to produce intense ultrashort pulses is a well-settled and understood technique [1], both from the theoretical and the experimental point of view. Among the systems that can act as saturable absorbers, we find dyes, SESAMs (semiconductor saturable absorber mirrors) [1] and, more recently, carbon nanotubes (CNTs)

and graphene. One advantage of the last two in relation to dyes and SESAMS is that they are not wavelength specific, so you can use the same absorber for a large variety of lasers. Carbon nanotubes have already been used to produce Q-switched [2] and mode-locked [3–6] laser pulses in bulk solid-state lasers. CNTs have been also used in fiber lasers using single-walled CNTs for the high-order harmonic mode locking [7] or single or double-walled CNTs for passive mode locking of erbium-doped fibers [8].

More recently, graphene has been employed for both temporal regimes, too, both in monolayer [9–11] and multilayer forms [12–14], in bulk solid-state lasers. While in fiber lasers, multilayer graphene [15] or graphene nanoparticles [16] have been used to produce mode locking in erbium-doped fiber lasers.

Both temporal regimes are not always easy to isolate experimentally from each other. Q-switch-modulated mode locking can appear or simply Q-switch can hinder mode locking. Hence, when looking for mode locking operation in a laser using a saturable absorber to produce ultrashort laser pulses, some attention should be paid to the possibility of Q-switched operation, which can make it more difficult to find pure mode locking. For example, the titanium:sapphire laser, which has optimal performance in mode locking, can be affected by the appearance of Q-switch in certain cavity designs [17–19]. In this paper, we want to evaluate the convenience of using carbon nanotubes or graphene in diode-pumped lasers, evaluating their performance as saturable absorbers for Q-switched operation. We will use as an example Nd:YLF laser. The choice of this type of laser is due, on one side, to the fact that it can be transversally pumped (side-pumped lasers have the advantage of a higher average output power) and, on the other side, because we have obtained good agreement between experimental and theoretical results in this type of laser in Q-switched operation using a monolayer graphene SAM [10].

2. The Model

In previous works, a model given by Haus and Spühler [20,21] has given good results when comparing experimental with simulated Q-switched operation using a monolayer G-SAM (graphene saturable absorber mirror) in a Nd:YLF laser [10] or predicting Q-switched operation in a short-cavity titanium:sapphire laser [19]. In this model, the intracavity power P, the gain g and the density of population inversion q can be calculated with the following set of equations [20,21]:

$$dP/dt = 1/t_r\,(g - l - q)\,P \tag{1}$$

$$dg/dt = -1/t_L\,((g - g_0) + gP/P_L) \tag{2}$$

$$dq/dt = -1/t_A\,((q - q_0) + qP/P_A) \tag{3}$$

where t_r is the cavity round-trip time; t_L, t_A the relaxation times of the laser medium and absorber, respectively; l the linear cavity losses; and P_L, P_A the saturation power of the laser medium and absorber. The meaning of g_0 and q_0 is explained below.

To compare the results obtained with graphene or carbon nanotubes as saturable absorbers deposited on a high-reflecting mirror (G-SAM or CNT-SAM), we have chosen a simple linear cavity (Figure 1), which employs of a Nd:YLF laser rod. Nd:YLF is a birefringent crystal, which has a thermal lens effect and can emit laser radiation at 1047 nm and 1053 nm with crossed polarizations, 1047 nm being the strongest line [22,23]. In our calculations, we used the λ = 1047 nm emission line, and the dimensions of the rod had typical values of $2a$ = 5 mm diameter, L_r = 5 cm length, refractive index 1.45.

The rod was placed in a plane-mirror resonator (SAM and output mirror (OM)) with a short physical length of 100 mm, corresponding to an optical length of L = 102.25 mm. Short-length cavities give shorter pulse durations, higher output powers and higher repetition rates in the Q-Switched regime [10,19] than longer ones.

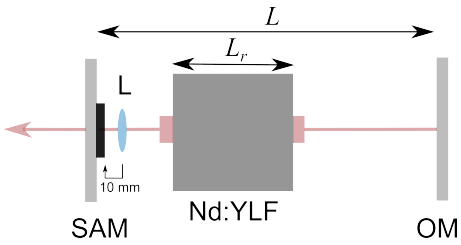

Figure 1. Cavity design for a transversally-pumped Nd:YLF laser. L: cavity length, L_r: laser rod length, L: focusing lens, OM: output mirror, SAM: saturable absorber mirror.

The SAM was considered to have a reflectivity R_{SAM} = 0.998 without the saturable absorber on it and the output mirror R_{OM} = 0.98. A lens L (f = 10 mm) was used to focus the laser beam onto the SAM to saturate the graphene or the CNTs. With this configuration, a stability analysis can be done where the thermal effects in the laser rod were introduced with a thermal lens with a focal length f = 200 mm. This analysis reveals that the TEM_{00} is practically collimated in the zone rod-OM and is strongly focused in the SAM. However, the geometry of the cavity has a high Fresnel number (*i.e.*, $\text{N}_F = a^2/(L\lambda) \sim 58$, for $a = 2.5$ mm, L = 102.25 mm, λ = 1047 nm), and we can assume transversal pumping, so it is more realistic to think of a multimode operation and estimate larger beam sizes at the rod and at the SAM than the values given at the stability analysis, which is done for the TEM_{00}. Hence, we have done the calculations estimating $w_r \sim 800$ μm at the rod and $w_{\text{SAM}} \sim 300$ μm at the SAM. This estimation is based on the fact that these orders of magnitude gave good results when comparing experimental and theoretical results in a transversally-pumped Nd:YLF [10].

Internal cavity losses were taken as $\alpha_i L_r$ = 0.1, which is a value within the typical order of magnitude for solid-state lasers, where α_i is the internal absorbance and L_r is the length of the laser rod. With these values, the linear cavity losses can be calculated as $l = 2(\alpha_i L_r - ln(R))$, being the average reflectivities given by $R = \sqrt{R_{\text{SAM}} R_{\text{OM}}}$. The quantity q_0 is the reflectivity change in the end mirror from absorbing to saturated absorber; this is the modulation depth. Carbon nanotubes have lower q_0 values than graphene. Modulation depths are typically around 1% and below [4–6], which correspond to q_0 = 0.01 and below. A single graphene layer absorbs ~2.3%; the absorbance of n graphene layers is $q_0 = -2n\, ln(1-0.023)$. Hence, with carbon nanotubes and mono- and multi-layer graphene, we can cover a large range in the parameter q_0. All graphene or nanotube layers were taken as uniform within the spot size of the beam at the SAM.

Other parameters, like relaxation times t_A for the absorber, saturation powers P_A and saturation fluences F_A, are more similar between graphene and carbon nanotubes. $t_A = 1.45$ ps for graphene [9], while t_A ranges from 0.75 ps to 1 ps for carbon nanotubes [4,6]. For graphene, F_{sat} is 14.5 μJ/cm^2 [9], while F_{sat} is 10 μJ/cm^2 for carbon nanotubes [4,6]. Therefore, it seems reasonable to choose for all parameters their values in graphene and to study just the influence of q_0.

Saturation powers for the absorber or the laser medium $P_{sat} = P_A, P_L$ were calculated from the saturation fluence F_{sat}. We used $P_{sat} = F_{sat}\pi w^2/\tau$, with τ the relaxation time of the laser medium ($t_L = 480$ µs [22]) and of the absorber ($t_A = 1.45$ ps [9]), w the beam waists at the laser rod (w_r) or at the SAM ($w_{\mathbf{SAM}}$), which, as mentioned, were estimated considering multimode operation. The saturation fluence for Nd:YLF is given by $F_{sat} = h\nu/(2\sigma)$, with h the Planck's constant, ν the laser emission frequency and σ the emission cross-section ($\sigma = 1.8 \times 10^{-19}$ cm^2 for the 1047-nm line of Nd:YLF [22]). g_0 is the unsaturated round-trip gain, and this parameter grows with increasing pumping intensity. We gave g_0 values ranging from 2- to 10-times the linear losses l, in steps of 1.

By solving Equations (1) to (3) using a 4th order Runge–Kutta method, we have studied the Q-switched regime (pulse duration, pulse energy and repetition frequency of the Q-switch train) as a function of g_0/l, for different values of q_0. The values chosen were $q_0 =$ 0.046 (two layers of graphene), 0.023 (one-layer of graphene) and 0.015, 0.01, 0.005 (representative values for CNTs) The integration time was always set long enough so that the stable regime (constant peak power) was reached. Tables 1 and 2 summarize the value of the parameters used in the calculations.

Table 1. Cavity parameters (see the text for details).

Laser Rod Diameter	Laser Rod Length	Refractive Index	Cavity Length	Output Mirror Reflectivity	SAM Reflectivity	Beam Waist at Laser Rod	Beam Waist at SAM
$2a$ = 5 mm	L_r = 5 cm	1.45	L = 100 mm	R_{OM} = 0.98	R_{SAM} = 0.998	ω_r = 800 µm	ω_{SAM} = 300 µm

Table 2. Laser and saturable absorber parameters (see the text for details).

Relaxation Times	Internal Cavity Losses	Saturation Fluences	Cavity Losses	Modulation Depth	Unsaturated Round-Trip Gain
t_L = 480 µs	$\alpha_i L_r$ = 0.1	$F_{sat} = h\nu/(2\sigma)$	$l = 2(\alpha_i L_r - ln(R))$	q_0 = 0.046, 0.023, 0.015, 0.010, 0.005.	g_0 = 2l to 10l
t_A=1.45 ps		$\sigma = 1.8\times10^{-19}$ cm^2			

Figure 2 shows the pulses obtained by integration of Equations (1) to (3) in the case q_0 = 0.015, g_0/l = 4, where it can be seen how the regime is stationary only after half a millisecond approximately.

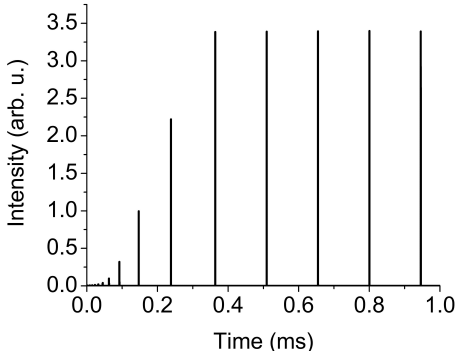

Figure 2. Q-switched regime obtained for $q_0 = 0.015$, g_0/l = 4.

The lower the value of q_0, the longer the integration time needed to reach the stationary Q-switched operation for low q_0/l values (for example, 5 ms, for q_0 = 0.005 and g_0/l = 2). Figure 3 is a temporal zoom on the last pulse of this train.

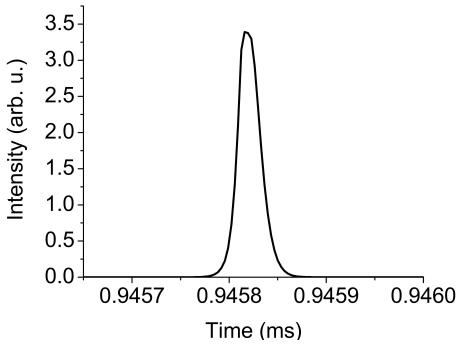

Figure 3. Temporal zoom in a Q-switched pulse in the train of Figure 2a obtained for $q_0 = 0.015$, $g_0/l = 4$.

In other cases, the temporal shape does not show a sharp peak, and the absorber is bleached for a longer time, giving rise to a flat-top-like temporal pulse, like in Figure 4, obtained for $q_0 = 0.046$ and $g_0/l = 4$.

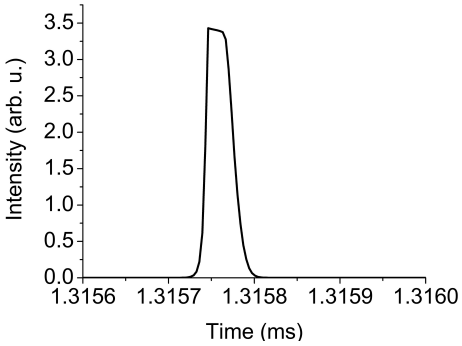

Figure 4. Temporal zoom in a Q-switched pulsed obtained for $q_0 = 0.046$, $g_0/l = 4$.

From this output, the temporal widths, the energy per pulse and the repetition rate can be deduced. Figure 5a shows the pulse durations obtained for q_0 ranging from 0.046 to 0.005. Very short pulse durations can be achieved in all cases, with very similar values with respect to g_0/l. The behavior is not monotonic and changes from $q_0 = 0.01$ to $q_0 = 0.005$. This behavior in the pulse duration is studied later in closer detail. Figure 5b shows the pulse energy obtained for the same range of q_0 values. Very high energies are obtained, and the highest values are obtained for the highest q_0. Like the pulse duration, the pulse energy does not depend significantly on the pump value g_0/l and remains practically constant for increasing pumping values from $g_0 = 2l$ to $g_0 = 10l$, being the unsaturated round-trip gain g_0 higher for higher pumping power. Figure 5c shows the repetition frequency of the pulse train and is the magnitude, which changes the most, increasing with g_0/l, and it is apparent that, unlike in the mode locking regime, the repetition rate in Q-switched operation mode is not fixed by the cavity round trip time. The lowest frequencies are obtained for the highest values of q_0. In Figure 5, the case $q_0 = 0.046$ for bilayer graphene and $g_0/l = 2$ did not reach Q-switch operation and extinguished after a couple of spikes.

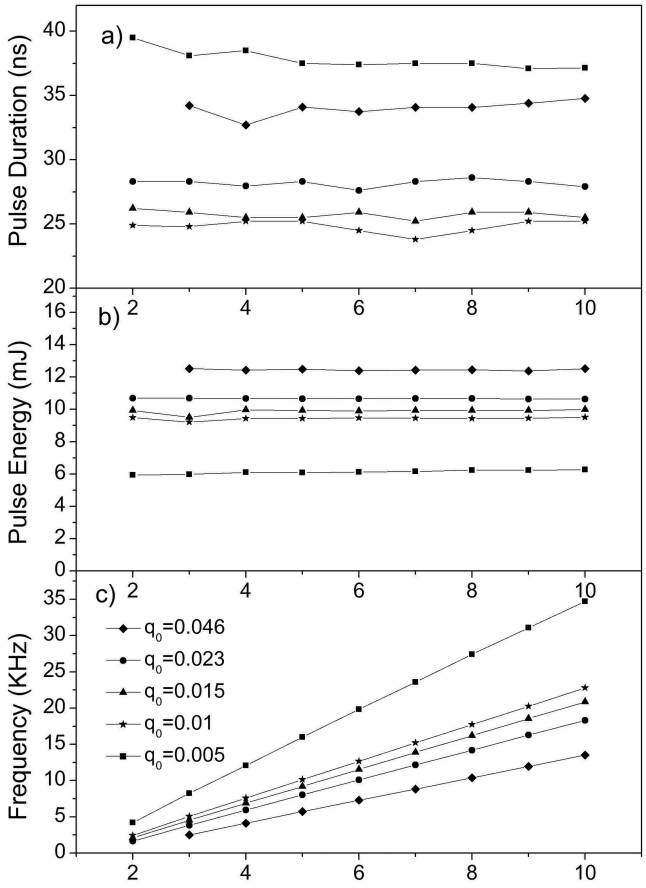

Figure 5. Pulse duration, pulse energy and repetition frequency for different absorptions g_0 as a function of the pump parameter g_0/l.

The behavior of the pulse duration and pulse energy has been studied in closer detail for g_0/l = 8 and an absorption range for the CNTs from $g_0 = 0.005$ to $g_0 = 0.01$ in steps of 0.001, as well as for monolayer and bilayer graphene. Figure 6a shows how the pulse duration reaches a minimum for $g_0 = 0.01$, while the pulse energy grows monotonically with q_0 in the whole range. According to the behavior of these two magnitudes in Figure 5a,b, which have a low dependence on g_0/l, the same behavior is expected for other values of g_0/l.

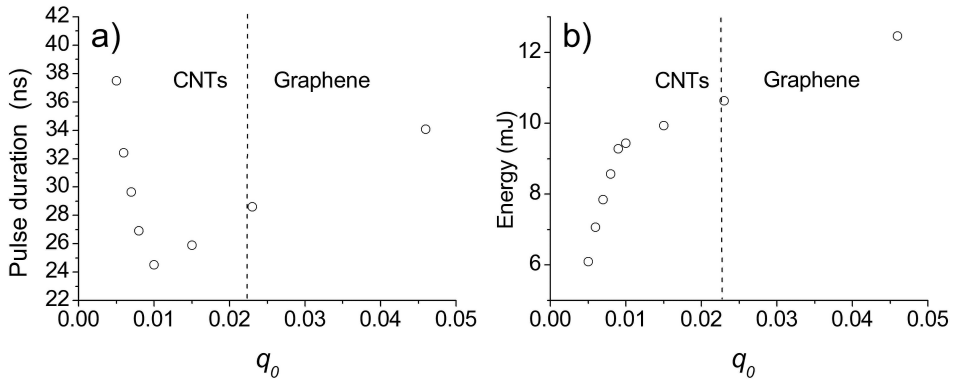

Figure 6. Pulse duration and pulse energy for g_0/l = 8 in an absorption range $g_0 = 0.005$ to $g_0 = 0.01$ in steps of 0.001 for CNTs, $g_0 = 0.023$ for monolayer graphene and $g_0 = 0.046$ for bilayer graphene.

Although the Q-switched regime is present in the range studied, when q_0 is very low (for example $q_0 = 0.001$), then only relaxation oscillations appear, tending to the cwstate for longer times (Figure 7).

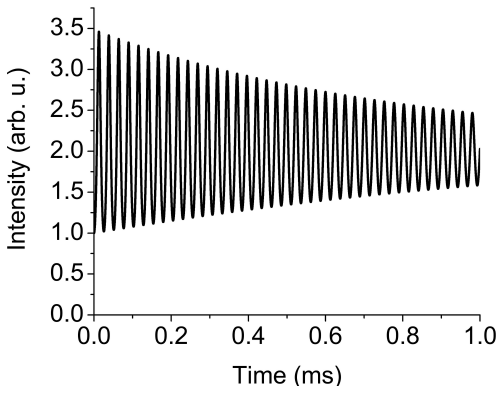

Figure 7. Relaxation oscillations obtained for $q_0 = 0.001$, g_0/l = 2.

3. Conclusions

Using a standard model, we have calculated the pulse duration, pulse energy and repetition rate of the Q-switched pulse train generated in a transversally-diode-pumped short-length cavity Nd:YLF laser using a graphene or CNT saturable absorber mirror. Higher energy pulses can be obtained for high values of the modulation depth q_0; this is for graphene. However, pulse duration reaches a minimum for a certain low q_0 value; this is for CNTs. Hence, when designing the laser, the choice of the proper q_0 must be done with a compromise between the desired energy and duration for the pulse. We have also observed that these two magnitudes do not depend significantly on the pump g_0/l for the geometry studied. The repetition rate of the train Q-switched pulses is higher for lower q_0 values and increases with the pump value g_0/l. The results also show that Q-switch can be hindered using CNTs with very low modulation depth ($\sim$0.001), the relaxation oscillations being the temporal regime in these cases. The results have certain universality and can be expected for other types of transversally-pumped short-length cavity lasers with an active medium with a lifetime in the order of hundreds of microseconds.

Acknowledgments

This work has been financed by the Universidad Complutense de Madrid through Project GR3/14-910133.

Author Contributions

José Manuel Guerra Pérez adapted and applied the model. Rosa Weigand programmed and solved the equations for the different cases and wrote the article. Margarita Sánchez Balmaseda processed the data.

Conflicts of Interest

The authors declare no conflict of interest.

References

1. Koechner, W. *Solid-State Laser Engineering*; Rhodes, W.T., Ed.; Springer Series in Optical Sciences; Springer: New York, NY, USA, 2006; pp. 522–528 and pp. 542–556.
2. Cheng, K.; Zhao, S.Z.; Yang, K.J.; Li, G.Q.; Li, D.C.; Zhang, G.; Zhao, B.; Wang, Y.G. Diode-pumped passively Q-switched Nd:$Lu_{0.33}Y_{0.37}Gd_{0.3}VO_4$ laser using a single-walled carbon nanotube saturable absorber. *Laser Phys. Lett.* **2011**, *8*, 418–422.
3. Set, S.Y.; Yaguchi, H.; Tanaka, Y.; Jablonski, M. Laser mode locking using a saturable absorber incorporating carbon nanotubes. *J. Lightwave Technol.* **2004**, *22*, 51–56.
4. Schibli, T.R.; Minoshima, K.; Kataura, H.; Itoga, E.; Minami, N.; Kazaoui, S.; Miyashita, K.; Tokumoto, M.; Sakakibara, Y. Ultrashort pulse-generation by saturable absorber mirrors based on polymer-embedded carbon nanotubes. *Opt. Express* **2005**, *13*, 8025–8031.
5. Schmidt, A.; Rivier, S.; Steinmeyer, G.; Yim, J.H.; Cho, W.B.; Lee, S.; Rotermund, F.; Pujol, M.C.; Mateos, X.; Aguiló, M.; *et al*. Passive mode locking of Yb:KLuW using a single-walled carbon nanotube saturable absorber. *Opt. Lett.* **2008**, *33*, 729–731.
6. Cho, W.B.; Schmidt, A.; Yim, J.H.; Choi, S.Y.; Lee, S.; Rotermund, F.; Griebner, U.; Steinmeyer, G.; Petrov, V.; Mateos, X.; *et al*. Passive mode locking of a Tm-doped bulk laser near 2 μm using a carbon nanotube saturable absorber. *Opt. Express.* **2009**, *17*, 11007–11011.
7. Cheng, K.; Lin, Y.; Yamashita, S.; Lin, G. Harmonic Order-Dependent Pulsewidth Shortening of a Passively Mode-Locked Fiber Laser With a Carbon Nanotube Saturable Absorber. *IEEE Photonics J.* **2012**, *4*, 1542–1552.
8. Cheng, K.; Lin, Y.; Lin, G. Single- and double-walled carbon nanotube based saturable absorbers for passive mode locking of an erbium-doped fiber laser. *Laser Phys.* **2013**, doi:10.10 88/1054-660X/23/4/045105.
9. Cho, W.B.; Kim, J.W.; Lee, H.W.; Bae, S.; Hong, B.H.; Choi, S.Y.; Baek, I.H.; Kim, K.; Yeom, D.; Rotermund, F. High-quality, large-area monolayer graphene for efficient bulk laser mode locking near 1.25 μm. *Opt. Lett.* **2011**, *36*, 4089–4091.
10. Matía-Hernando, P.; Guerra, J.M.; Weigand, R. An Nd:YLF laser q-switched by a monolayer-graphene saturable-absorber mirror. *Laser Phys.* **2013**, doi:10.1088/1054-660X/23/2/025003.
11. Xie, G.Q.; Ma, J.; Lv, P.; Gao, W.L.; Yuan, P.; Qian, L.J.; Yu, H.H.; Zhang, H.J.; Wang, J.Y.; Tang, D.Y. Graphene saturable absorber for Q-switching and mode locking at 2 μm wavelength. *Opt. Mater. Express* **2012**, *2*, 878–883.
12. Li, X.L.; Xu, J.L.; Wu, Y.Z.; He, J.L.; Hao, X.P. Large energy laser pulses with high repetition rate by graphene Q-switched solid-state laser. *Opt. Express* **2011**, *19*, 9950–9955.
13. Wang, Z.T.; Zou, Y.H.; Chen, Y.; Wu, M.; Zhao, C.J.; Zhang, H.; Wen, S.C. Graphene sheet stacks for Q-switching operation of an erbium-doped fiber laser. *Laser Phys. Lett.* **2013**, doi:10.1088/1612-2011/10/7/075102.
14. Husaini, S.; Bedford, R.G. Graphene saturable absorber for high power semiconductor disk laser mode locking. *Appl. Phys. Lett.* **2014**, doi:10.1063/1.4872258.

15. Huang, P.L.; Lin, S.; Yeh, C.; Kuo, H.; Huang, S.; Lin, G.; Li, L.; Su, C.; Cheng, W. Stable mode-locked fiber laser based on CVD fabricated graphene saturable absorber. *Opt. Express* **2012**, *20*, 2460–2465.
16. Lin, Y.; Yang, C.; Liou, J.; Yu, C.; Lin, G. Using graphene nano-particle embedded in photonic crystal fiber for evanescent wave mode locking of fiber laser. *Opt. Express* **2013**, *21*, 16763–16776.
17. Sali, E.; Ignesti, E.; Cavalieri, S.; Fini, L.; Tognetti, M.; Bu, R. A tuneable, single-mode titanium-doped-sapphire laser source with variable pulse duration in the nanosecond regime. *Opt. Commun.* **2009**, *282*, 3330–3334.
18. Sali, E.; Ignesti, E.; Cavalieri, S.; Fini, L.; Tognetti, M.; Bu, R. A titanium-doped-sapphire laser source with tunable frequency, single-mode emission, and adjustable pulse duration. *Laser Phys.* **2010**, *20*, 1126–1131.
19. Weigand, R.; Pinto, T.; Crespo, H.M.; Guerra, J.M. On the Q-switched operation of Titanium: Sapphire lasers using a graphene-based saturable absorber mirror. *Opt. Laser Technol.* **2015**, *72*, 1–5.
20. Spühler, G.J.; Paschotta, R.; Fluck, R.; Braun, B.; Moser, M.; Zhang, G.; Gini, E.; Keller, U. Experimentally confirmed design guidelines for passively Q-switched microchip lasers using semiconductor saturable absorbers. *J. Opt. Soc. Am. B* **1999**, *33*, 376–388.
21. Haus, H. Parameter ranges for cw passive mode locking. *IEEE J. Quantum Electron.* **1976**, *12,* 169–176.
22. Pollack, T.M.; Wing, W.F.; Grasso, R.J.; Chicklis, E.P.; Jenssen, H.P. Cw laser operation of Nd:YLF. *IEEE J. Quantum Electron.* **1982**, *18*, 159–163.
23. Frei, B.; Balmer, J.E. 1053-nm-wavelength selection in a diode-laser-pumped Nd:YLF laser. *Appl. Opt.* **1994**, *33*, 6942–6946.